Supplement of Weather Clim. Dynam., 6, 431–446, 2025
https://doi.org/10.5194/wcd-6-431-2025-supplement

Supplement of

Moisture transport axes: a unifying definition for tropical moisture exports, atmospheric rivers, and warm moist intrusions

Clemens Spensberger et al.

Correspondence to: Clemens Spensberger (clemens.spensberger@uib.no)

S1 Moisture transport axes based on normalised input data

The frequent detection of moisture transport axes at low latitudes (climatology in Fig. 3 in the main manuscript) indicates that also many less impactful events, such as seasonal or even stationary features of the circulation, are detected. For some applications, however, it might be desirable to limit detections to the most pronounced moisture filaments at low latitudes. In the following, we explore the potential benefits of normalising the IVT input fields to achieve more selective detections at low latitudes.

For this analysis, we normalised the IVT by the annual and zonal mean total column water vapour $\overline{\text{TCWV}}$ (black dashed lines in Fig. S1 show resulting detections, climatology in Fig. S2). For brevity, we refer to these as "normalised detections", in contrast to the "non-normalised" detections discussed in the main manuscript. Given that the non-normalised detections are tuned with a particular focus on the storm tracks, we aim to keep detections in these regions unchanged by the normalisation. We achieve this by defining the normalised IVT_n by

$$\text{IVT}_n = \text{IVT}\frac{\overline{\text{TCWV}}(40°\text{N/S})}{\max(\overline{\text{TCWV}}_{\text{min}}, \overline{\text{TCWV}})}$$

and using IVT_n instead of IVT as input to the detection algorithm, while keeping the K_{IVT}-threshold unchanged. The annual zonal mean $\overline{\text{TCWV}}(40°\text{N/S}) \approx 18\,\text{kg}\,\text{m}^{-2}$ and we set a minimum $\overline{\text{TCWV}}_{\text{min}} = 3\,\text{kg}\,\text{m}^{-2}$ to avoid detections rates that well exceed the ones reported by Wille et al. (2021) over the extremely dry Antarctic continent. With the minimum $\overline{\text{TCWV}}_{\text{min}} = 3\,\text{kg}\,\text{m}^{-2}$, we suppress essentially all detection over the interior of the Antarctic continent, but one might be able to recover the atmospheric rivers discussed by Wille et al. (2021) by lowering this threshold. We considered alternative normalisation by the (zonally asymmetric) annual mean TCWV as well as the seasonal mean TCWV, but the results are qualitatively very similar (not shown).

S1.1 Case studies from low, mid, and high latitudes

In the case studies, the most prominent moisture filaments are detected both with and without normalisation (compare dashed black and yellow lines in Fig. S1). This is true also beyond the mid-latitudes (e.g., around monsoon cyclone in the Gulf of Bengal in Fig. S1 and the atmospheric river making landfall on Antarctica studied by Gorodetskaya et al. (2014) in Fig. S1). Within the mid-latitudes, the cases exhibit only minor differences between normalised and non-normalised moisture transport axes. This is expected, as we constructed our normalisation such to leave mid-latitude detections generally unchanged.

Nevertheless, there are clearly more (fewer) detections of transport axes at high (low) latitudes with the normalised detections. Analogously, normalised transport axes trace the moisture filament over longer (shorter) distances in the Arctic (subtropics and tropics). For example, the weaker polar moisture filament associated with the cyclone in the Canadian Arctic in Fig. S1 is only detected with normalisation. Vice-versa, the relatively stationary Somali Jet and moisture flow across the Indian Ocean in Fig. S1f is only detected as a moisture transport axes if the input is not normalised.

S1.2 Climatology of normalised detections

Climatologically, most tropical and subtropical detections vanish with normalisation (Fig. S2). The remaining moisture transport axes are associated with the South American low-level jet or with the Somali Jet and Indian Monsoon during the monsoon season (Fig. S2c). For the remainder of the subtropics and tropics, detections are limited to the most pronounced moisture filaments, which generally occur at less than 5% of the time steps for all seasons.

At the same time, more moisture transport axes are detected in polar regions. With normalisation, the 5%-isoline touches the Antarctic continent year-round, and the 1%-isoline is generally 100-200 km onshore. (Fig. S2). Similarly, in the North Atlantic, the detections during winter around 70° increase by around a factor of three, from approx. 5% to approx. 15% frequency of occurrence. Further, along the West Greenland coast, a normalised moisture transport axis occurs 1.0-2.5% of the time steps year-round. Thus, with normalisation, moisture transport axes start to occur in the drier Arctic climates, whereas they become an event of everyday weather in moister polar regions such as the Atlantic Arctic.

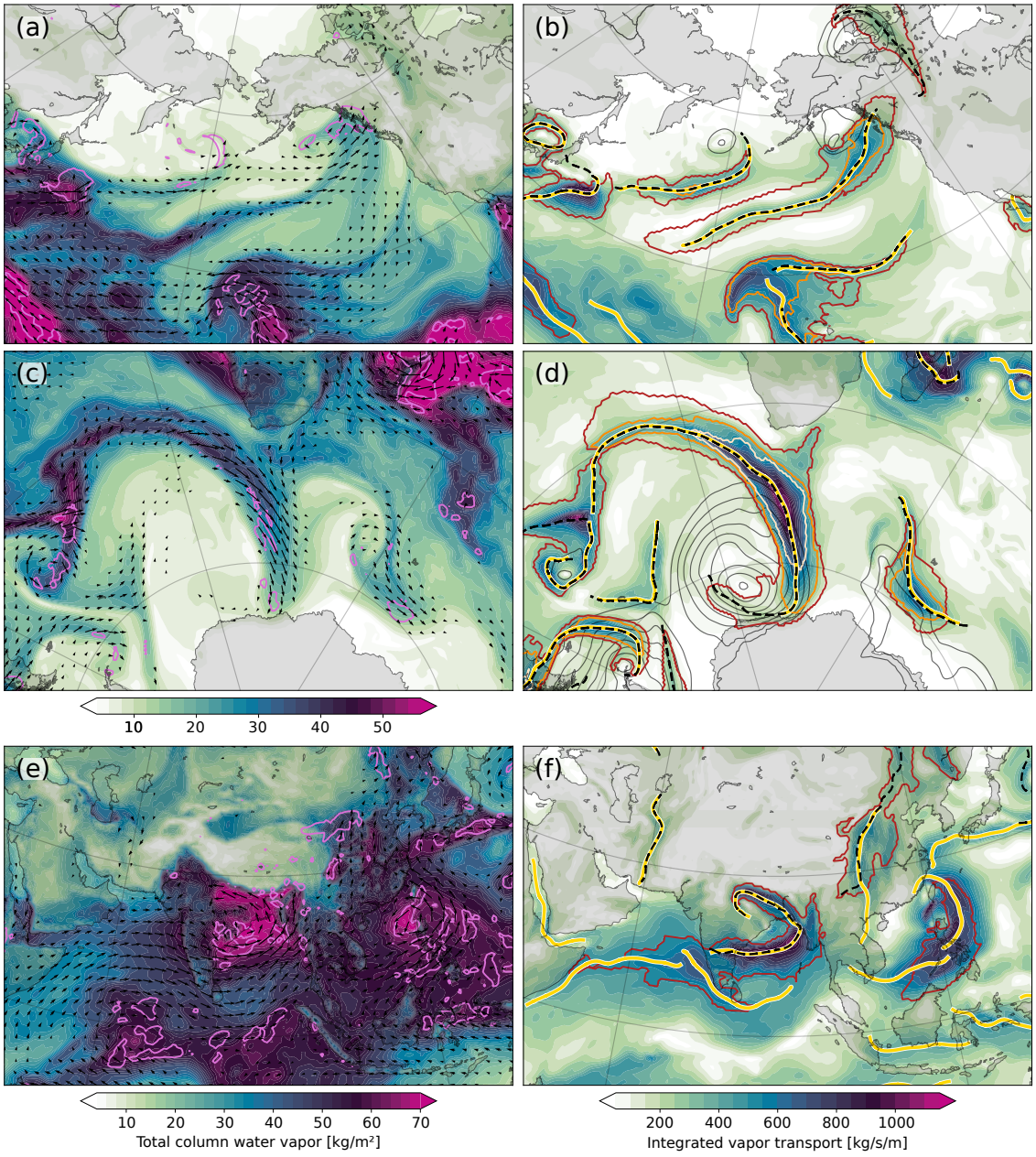

Figure S1. As Fig. 2 in the main manuscript, but in addition also showing normalised moisture transport axes (dashed black lines). The rows show (a,b) the other atmospheric river case discussed in Rutz et al. (2019), (c,d) the other atmospheric river case discussed in Gorodetskaya et al. (2014), and (e,f) an snapshot from the 2012 Indian Monsoon. The rows show (a,b) 23 October 2006, 12Z, (c,d) 15 February 2011, 00Z, and (e,f) 20 July 2012, 18Z.

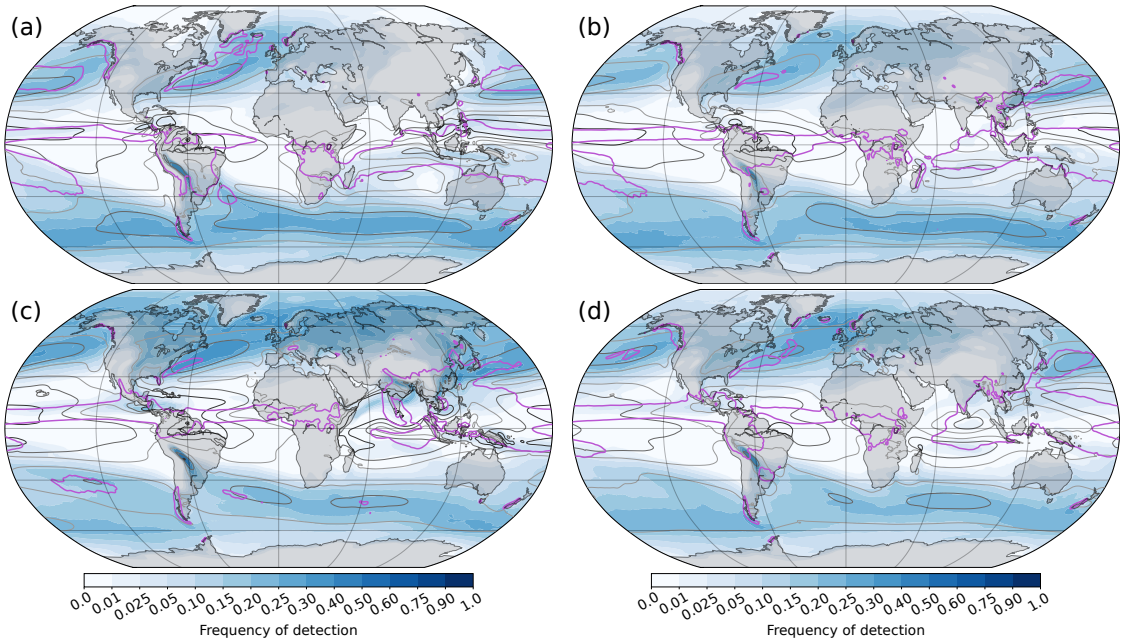

Figure S2. As Fig. 3 in the main manuscript, but for the normalised moisture transport axes.

S1.3 Normalised moisture transport axes in the subtropics

For the Indian Monsoon, normalisation reduces the number of detected events to about half (Fig. S3a,b). A moisture transport axis is thus present in the vicinity of Kolkata for about 30% of the time steps during the monsoon season. This frequency is similar to the peak occurrence of moisture transport axes in the North Atlantic, which just exceeds 25% during winter (Fig. S2a; Fig. 3a in the main manuscript). Normalisation thus isolates particularly pronounced moisture transport events within the otherwise relatively stationary monsoon circulation.

This conclusion is supported by the similar but clearer synoptic structure evident in the normalised composites (compare Fig. S3 with Fig. 9 in the main manuscript). The atmosphere is even more loaded with water and precipitation is even more widespread. Further, the moisture transport features a closed cyclonic circulation over the Indian subcontinent (Fig. S3a). Upstream, a larger region exceeds an IVT of $300\,\mathrm{kg\,s^{-1}\,m^{-1}}$ (darkest grey contour in Fig. S3b), while fewer transport axes connect the Indian monsoon to the Somali Jet. This further indicates that the normalised composite emphasises a regional/synoptic intensification of the Monsoon circulation over India.

Analogously, the extrusion of tropical moisture towards the Sahel region is much more pronounced in the normalised composite (compare Fig. S3c and Fig 9c in the main manuscript) and features pronounced moisture transport across the Sahel and towards the northeast, crossing the Sahara into the Mediterranean. The tilted structure seen in the mean moisture transport is reflected in both normalised and non-normalised transport axis detections (Fig. S3b,d), indicating that both the normalised and the non-normalised composites capture the same synoptic phenomenon, while the normalised composite only includes the most pronounced events.

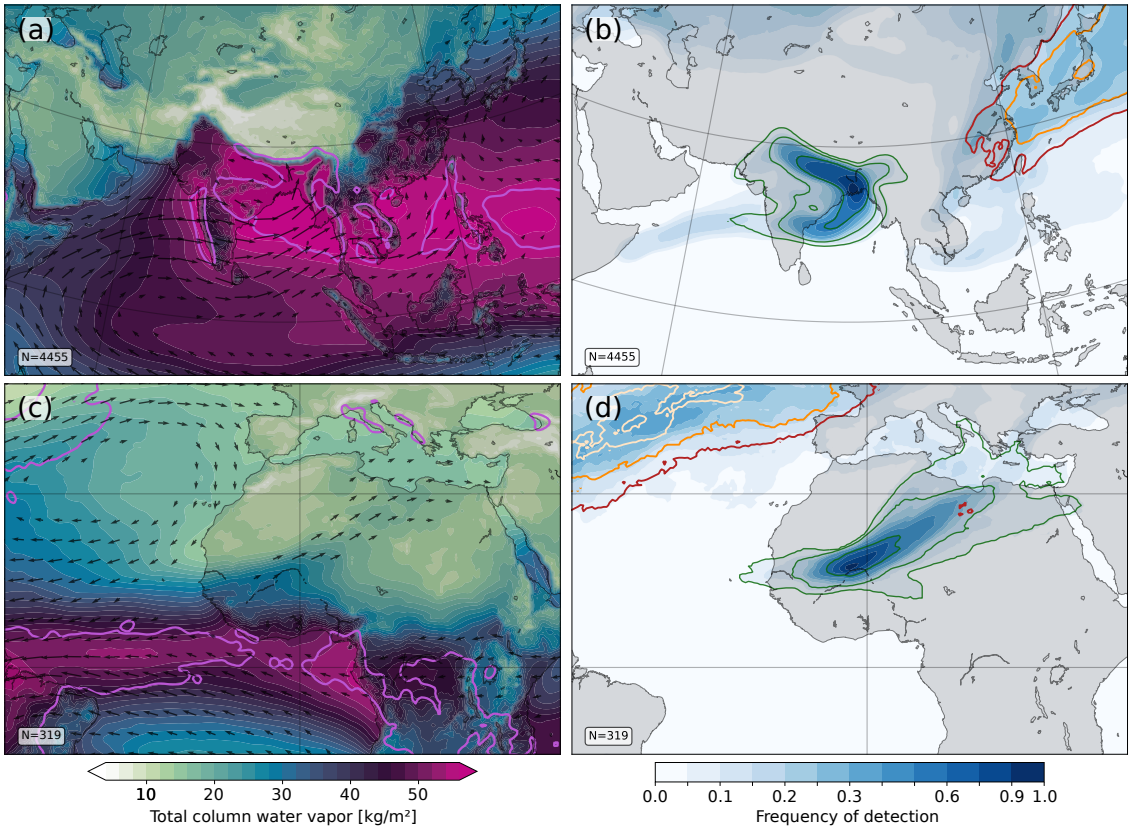

Figure S3. As Fig. 9 in the main manuscript, but for normalised moisture transport axes.

References

Gorodetskaya, I. V., Tsukernik, M., Claes, K., Ralph, M. F., Neff, W. D., and Van Lipzig, N. P. M.: The role of atmospheric rivers in anomalous snow accumulation in East Antarctica, Geophysical Research Letters, 41, 6199–6206, https://doi.org/10.1002/2014GL060881, 2014.

Rutz, J. J., Shields, C. A., Lora, J. M., Payne, A. E., Guan, B., Ullrich, P., O'Brien, T., Leung, L. R., Ralph, F. M., Wehner, M., Brands, S., Collow, A., Goldenson, N., Gorodetskaya, I., Griffith, H., Kashinath, K., Kawzenuk, B., Krishnan, H., Kurlin, V., Lavers, D., Magnusdottir, G., Mahoney, K., McClenny, E., Muszynski, G., Nguyen, P. D., Prabhat, M., Qian, Y., Ramos, A. M., Sarangi, C., Sellars, S., Shulgina, T., Tome, R., Waliser, D., Walton, D., Wick, G., Wilson, A. M., and Viale, M.: The Atmospheric River Tracking Method Intercomparison Project (ARTMIP): Quantifying Uncertainties in Atmospheric River Climatology, Journal of Geophysical Research: Atmospheres, 124, 13 777–13 802, https://doi.org/10.1029/2019JD030936, 2019.

Wille, J. D., Favier, V., Gorodetskaya, I. V., Agosta, C., Kittel, C., Beeman, J. C., Jourdain, N. C., Lenaerts, J. T. M., and Codron, F.: Antarctic Atmospheric River Climatology and Precipitation Impacts, Journal of Geophysical Research: Atmospheres, 126, e2020JD033 788, https://doi.org/10.1029/2020JD033788, 2021.